Optics Communications 282 (2009) 1496–1500

Contents lists available at ScienceDirect

Optics Communications

journal homepage: www.elsevier.com/locate/optcom

Retina imaging system with adaptive optics for the eye with or without myopia

Chao Li [a,b,*], Mingliang Xia [a,b], Baoguang Jiang [a,b], Quanquan Mu [b], Shaoyuan Chen [a,b], Li Xuan [b]

[a] Graduate School of the Chinese Academy of Sciences, Beijing 100039, China
[b] State Key Lab of Applied Optics, Changchun Institute of Optics, Fine Mechanics and Physics, Chinese Academy of Sciences, Changchun, Jilin 130033, China

ARTICLE INFO

Article history:
Received 10 March 2008
Received in revised form 20 November 2008
Accepted 19 December 2008

Keywords:
Adaptive optics
Ophthalmic optics
Retina imaging

ABSTRACT

An adaptive optics system for the retina imaging is introduced in the paper. It can be applied to the eye with myopia from 0 to 6 diopters without any adjustment of the system. A high-resolution liquid crystal on silicon (LCOS) device is used as the wave-front corrector. The aberration is detected by a Shack–Hartmann wave-front sensor (HASO) that has a Root Mean Square (RMS) measurement accuracy of $\lambda/100$ ($\lambda = 0.633$ μm). And an equivalent scale model eye is constructed with a short focal length lens (~18 mm) and a diffuse reflection object (paper screen) as the retina. By changing the distance between the paper screen and the lens, we simulate the eye with larger diopters than 5 and the depth of field. The RMS value both before and after correction is obtained by the wave-front sensor. After correction, the system reaches the diffraction-limited resolution approximately 230 cycles/mm at the object space. It is proved that if the myopia is smaller than 6 diopters and the depth of field is between −40 and +50 mm, the system can correct the aberration very well.

1. Introduction

The optical system of human eyes is often far from the diffraction-limited. In everyday life, the brain compensates for the image formation defects, so that the world representation appears sufficiently sharp and we can get a clear scene of the world. Nevertheless, for eye fundus examinations, the eye's optical aberration reduces the image resolution severely. For many clinical applications and psychophysical experiments, ophthalmologists cannot obtain the maximum resolution that they may need. As early as 1961, Smirnov [1] proposed to correct higher order aberrations of the eye, and he provided a description of the third and fourth order aberrations by employing a subjective vernier task to measure the retinal misalignment of rays that are entering through different parts of the pupil. Following Smirnov's pioneering work [2], a number of investigators devised a variety of different methods to characterize the wave-front aberration of human eye. In 1994 [3], Liang and Williams first measured eye aberrations up to the fourth Zernike order with a Shack–Hartmann wave-front sensor and then to the tenth Zernike order. This was proved to be the key development that paved the way to closed-loop adaptive optics systems for the eye. In 1997, Liang et al. successfully build an adaptive optics system for high-resolution retinal imaging based on the technique of Shack–Hartmann wave-front sensor [4]. Later on some other research teams have implemented AO systems with deformable mirror as the wave-front corrector for retinal imaging [5–7]. High-resolution retinal imaging has found a home in vision science, where it is used by a number of researchers to further our understanding on the human retina.

One of the most exciting applications of adaptive optics is in the diagnosis and treatment of retinal disease [8]. The advantage offered by AO is that the microscopic structure of the diseased retina can be imaged in vivo and tracked in a single eye, monitoring the progression of the disease or the efficacy of the therapy over the time. But all current adaptive optical systems for retinal imaging are accommodated for the normal eyes [5–7]. So, the AO systems can only be applied to the human eyes with good vision. The conventional AO system cannot be applied to the eye with large myopia, which will induce very large defocus aberration. Although the problem can be resolved by using a movable four mirror sub system (Badal system) [9,10], it makes the system complex. Thibos and Bradley [11] have reported about the correction of spherical and astigmatic refractive changes in the eye with about 1.5 diopters with 127 liquid crystal cells, and some other investigators have managed to use liquid crystal phase modulator to correct the aberration of eyes [12,13]. But it cannot correct large aberration yet. In this paper, we demonstrate a novel AO system for retinal imaging with high-resolution LCOS as the corrector and with a model eye as the object. Our experiments proved that the AO system can perfectly correct the aberration for the eye with myopia from 0 to 6 diopters and even to 8 diopters. And it might well correct the eye aberration from 0 to 10 diopters by adjusting some of the optical elements.

* Corresponding author. Address: State Key Lab of Applied Optics, Changchun Institute of Optics, Fine Mechanics and Physics, Chinese Academy of Sciences, Changchun, Jilin 130033, China.
E-mail address: nk_lich@hotmail.com (C. Li).

0030-4018/$ - see front matter © 2008 Elsevier B.V. All rights reserved.
doi:10.1016/j.optcom.2008.12.048

2. Instruments setup

The model eye consisted of a short focal length lens L1 and a white paper screen adhered with toner granules. The effective focal length of lens L1 is 18 mm (±2%), which is almost equivalent to the focal length of human eye [14]. The toner granules are blown up, and then they fall on a piece of paper dispersedly. The size of the toner granules distributes from 4 to 10 μm as shown in Fig. 1. The left-up picture in Fig. 1 is the image of the resolution target (Standard USAF), and the smallest lines in its seventh group are 228 cycles/mm. It should be emphasized that the two pictures are taken with the same zoom ratio. Here, the paper can be taken as the retina, and the toner granules can be taken as the cells. What's more, the distance between the lens and paper is about 20 mm, so that the paper will conjugate with the plane at 200 mm distance on the other side of the lens. In this case, the model eye is staring at the object that is 200 mm away. Because the focal length of lens L1 is not very accurately measured and a little deviation of the distance between lens L1 and the paper will induce a large deviation of the conjugate distance, we made fine adjustment for the paper position to ensure that its conjugated distance is 200 mm in the experiment. Although the model eye is static, it has the 1:1 scale as the real eye, and it will be sufficient to simulate the defocus of the eye which will be very large for most conditions.

S1 is the target light source (white light, 1 mm diameter). The optical path between S1 and lens L1 is 200 mm, which is the same as the optical path from L1 to the point S1', i.e. S1 and S1' are optically conjugated. Because the "eye" is focused on S1, the light reflected out of the "eye" will focus at S1'. So, the point S1' is the first real image of the retina. The "retina" illuminated source is the light spot on laser diffuser P1, which is also used as the reference source for wave-front measurement in the principle experiment. In order to control the size of the illuminated area on the paper screen about 0.1 mm, the size of light spot P1 and the distance between P1 and lens L1 will be adjusted for the "eye" with different diopters. Originally, the diameter of the light spot P1 is about 1 mm, and the distance between P1 and lens L1 is about 200 mm. It is certainly that S1 will be useless for the model eye but very important for the real eye.

Concave lens L2 change the focusing light reflected from the "eye" into parallel light beam. And the virtual image of the mimetic pupil P2 after L2 is just at the focal plane of lens L3. The size of "pupil" P2 is 6 mm. Lens L3 and L4 make the virtual image of the "pupil" conjugate with the corrector LCOS (pixel pitch: 19 × 19 μm; pixel number:1024 × 768). Lens L4 and L5 make LCOS conjugate with the Shack–Hartmann wave-front sensor HASO (aperture:5 × 5 mm; sub-aperture number:32 × 32). So, we can make the "pupil of the eye" conjugate with LCOS and HASO and at the same time the ideal incidence light into HASO will be plane wave. It is necessary to use polarizer P3 to convert the non-polarized light into appropriate polarized light because LCOS can only operate on linear-polarized light [15,16].

The illuminating light source that we used in the experiment is a commercial laser diode (LD) with output wavelength 532 nm. The laser diffuser can successfully eliminate the laser speckle as shown in Fig. 2. Fig. 2a shows the image of the paper illuminated by the 532 nm laser directly, Fig. 2b shows the image of the paper illuminated by the laser after diffuser P1 and Fig. 2c shows the image of the paper illuminated by white light. The effect of laser illuminating after the diffuser is the same as that of the white light.

3. Experiment methods

Firstly, we adjust the optical system to the ideal state, i.e. the first real image of the paper made by lens L1 is at right point S1'. Because Lens L4 is abaxial about 3 mm, the incidence light wave represents coma aberration just as shown in Fig. 3.

Actually, the human eye can automatically adjust the power of its optical system to accommodate the staring point, so that either far object or near object can form a clear image on the retina. But it is impossible to adjust the power of a glass lens discretionarily. As a result, we adjust the distance between the paper screen and lens L1 to simulate the "eye" with large diopters. For example, when we move the paper a little farther from lens L1, the conjugated plane of the paper will move towards L1, which is just like the diopter larger and the staring point nearer.

We know that the myopia eye above 5 diopters cannot accommodate the focusing point farther than 200 mm, because the most distant staring point for the eye with D diopters myopia is only $1000/D$ mm away. So, the myopia eye above 5 diopters cannot focus on the 200 mm far point no matter how to adjust the power of the eye. On the contrary, the eye with good vision or below 5 diopters can adjust to focus on the point at 200 mm away easily. So in the experiment, we move the paper screen farther by farther from L1 to simulate high diopter myopia eye. Fig. 4 shows the relationship between diopters and the backward distance (denoted by "−"). For example, when moving the paper screen backwards 0.4 mm (i.e. the distance between paper screen and lens L1 is 20.4 mm), the conjugated position of the paper screen is 166 mm far from lens L1, and the corresponding diopter is 6.

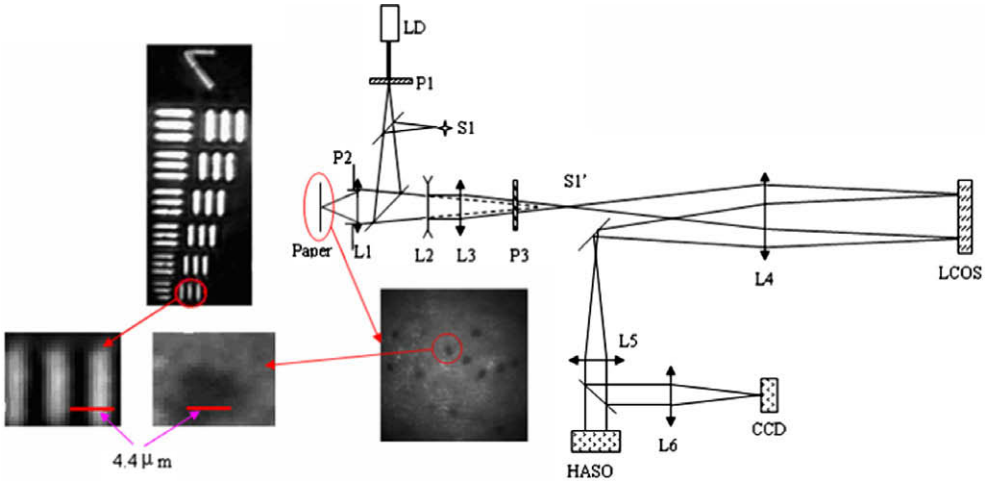

Fig. 1. The configuration of the optical system.

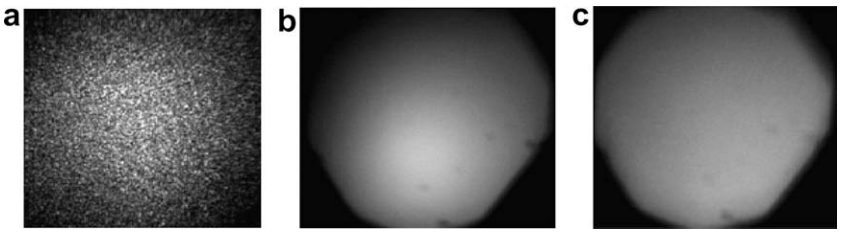

Fig. 2. (a) Laser illuminates directly; (b) laser illuminates after diffuser; (c) white light illuminates.

The depth of field exists in every optical system including human eye, so that when we see the object at 200 mm away clearly the actual distance may be larger or smaller than 200 mm. The depth of field is only 2 mm when focusing 200 mm away and the size of pupil is 6 mm. Here, we redefine the depth of field as the depth of view, i.e. the difference between 200 mm and the actual position of the staring point (i.e. the conjugated plane of the paper) after moving the paper. The depth of view is exaggerated to several tens millimeters. Fig. 5 shows the relationship between the depth of view and the moving distance (backward ones donated by "−" and forward ones donated by "+"). For example, when the paper moves towards lens L1 +0.1 mm, the conjugated position of the paper screen is at 189 mm away from lens L1 and the depth of view is −11 mm.

The optical system shown in Fig. 1 can be looked as a microscope system illuminated vertically. By Rayleigh's criterion, the smallest separation between two object points that will allow them to be resolved is given by [17]

$$Z = \lambda/\mathrm{NA} \quad \text{and} \quad \mathrm{NA} = n^* \sin U, \quad U = D_p/(2l_0)$$

where λ is the wavelength, and NA is the object space numerical aperture. Both the index n and the slope of the marginal ray U are at the object space. D_p is the diameter of pupil, and l_0 is the distance between the screen paper and lens L1. So, the smallest separation will change when moving the paper screen, which is shown in Fig. 6. But we will ignore the change due to the maximum difference, which is only 0.15 μm (7.5%) according to Fig. 6.

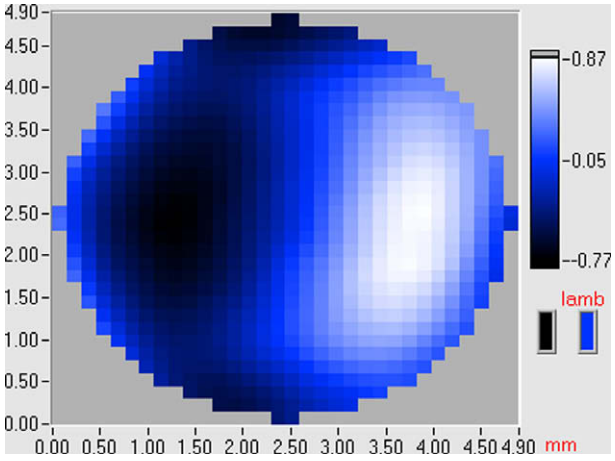

Fig. 3. The initial wave-front map obtained by HASO.

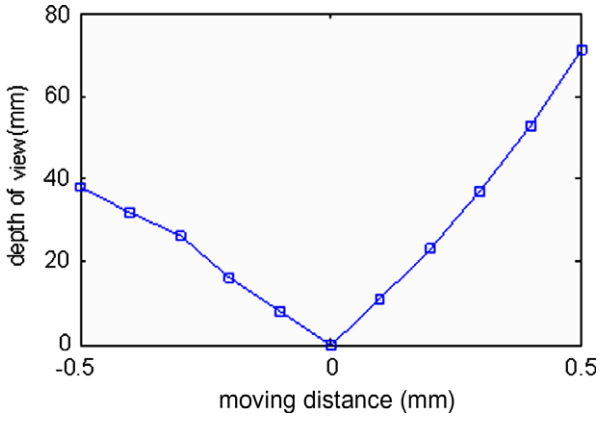

Fig. 5. The relationship between the depth of view and the moving distance of the paper-screen.

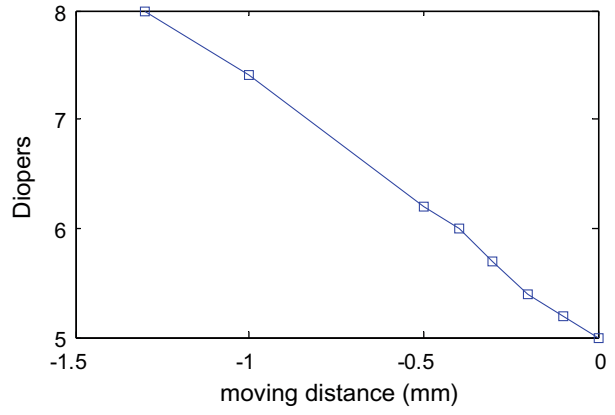

Fig. 4. The relationship between diopters and backward distance of the paper screen (when pupil size is 6 mm).

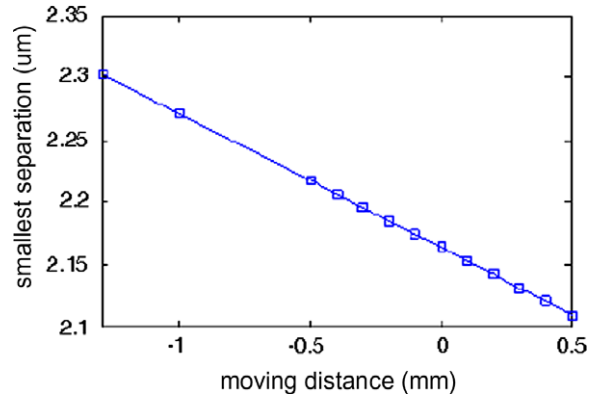

Fig. 6. The relationship between the smallest separation and the moving distance.

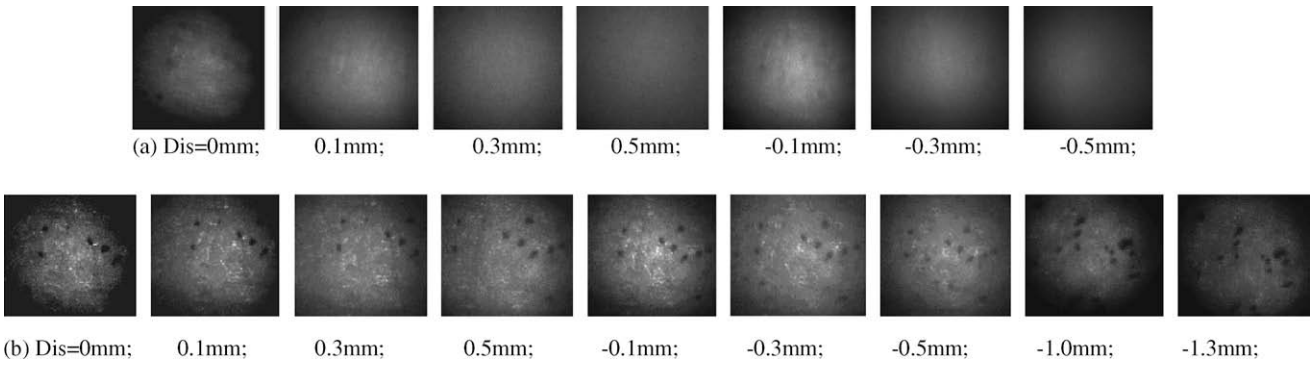

Fig. 7. When moving the paper screen, we get the images as shown above: (a) shows the images before aberration is corrected and (b) shows the images after correction. The black stains are the toner granules that are about 5 μm.

4. Results and discussion

When moving the paper screen backward or forward with a 0.1 mm step size, the wave-front aberration tested by HASO increases quickly and the images of the paper screen turn more and more obscure as shown in Fig. 7a. The RMS values of the wave-front measured by HASO reach several wavelengths (Fig. 9a), and the main component of the aberration is defocus, which can be seen from the wave-front map Fig. 8).

After correction, the RMS values reduce to 0.1λ or smaller (Fig. 9b), when the moving distance is between −0.5 and +0.5 mm. At the same time, all the images after correction turn clear as it is shown in Fig. 7b. But when the moving distance reaches −1.0 mm and −1.3 mm, the RMS value of residual wave-front aberration after correction is still above 0.1λ because the initial wave-front aberration is too large (RMS value is about 5λ, and the peak-to-valley value is about 20λ). Finally, we take the image of the resolution target (Standard USAF, shown in Fig. 10) after correction when the moving distance is zero (Dis = 0 mm) in order to testify the resolution capability of the system. The spatial frequency of the seventh group is listed in Table 1.

Taking the relationship between the moving distance and diopters (Fig. 4) and the depth of view (Fig. 5) into consideration, we can conclude that when the diopter is smaller than 6 the system can perfectly correct the wave-front aberration, otherwise the aberration will be too large to be corrected totally. Besides, even if the depth of view reaches ±30 mm, the system can compensate the aberration successfully.

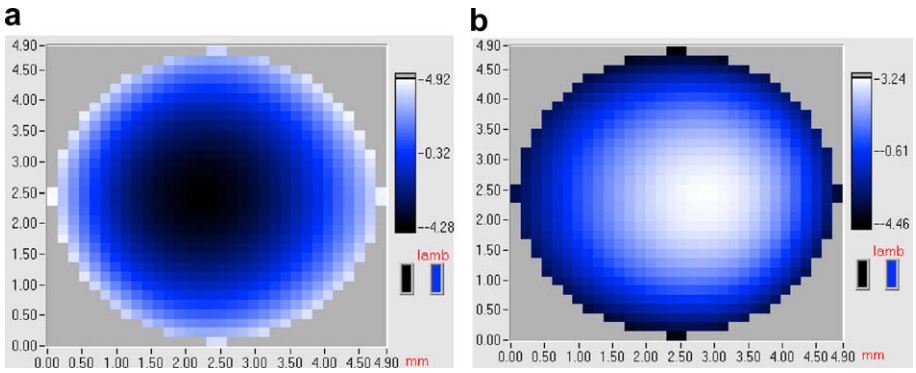

Fig. 8. (a) The wave-front map when Dis = 0.3 mm; (b) the wave-front map when Dis = −0.3 mm.

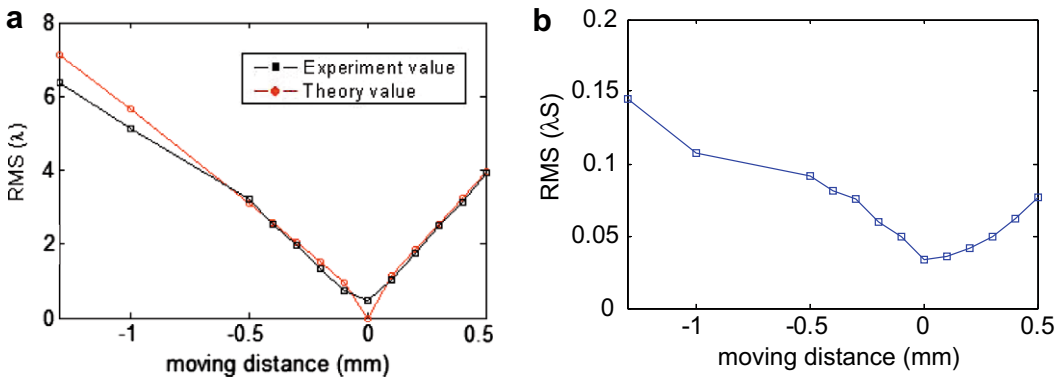

Fig. 9. (a) RMS value before correction; (b) RMS value after correction.

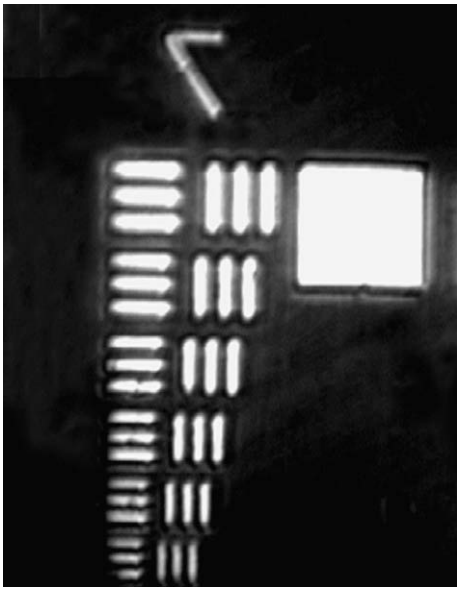

Fig. 10. The resolution target image after correction.

Table 1
Resolution value of Standard USAF 1951 resolution test pattern (unit: cycles/mm).

Elements no.	7.1	7.2	7.3	7.4	7.5	7.6
Resolution value	128	143	161	181	203	228

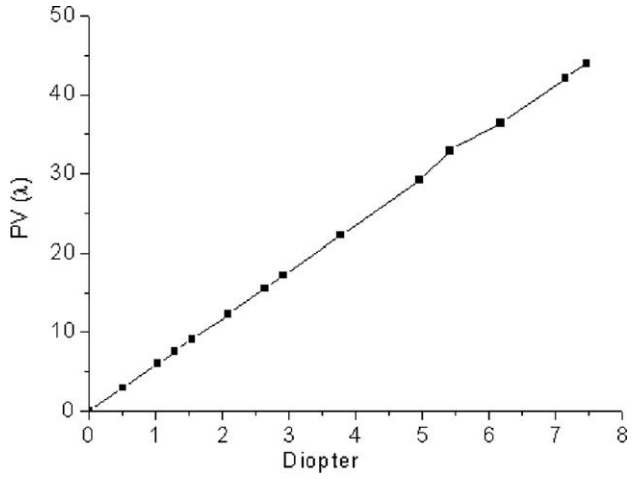

Fig. 11. PV value of the aberration due to the diopter for the common AO system for retina imaging (pupil size is 6 mm, and zoom ratio between pupil and S-H WFS is 6:5).

At last, we calculate the PV value of the wave-front aberration with different diopters (the pupil size is set 6 mm, and the zoom ratio between pupil and HASO is 6:5) for the target at infinity, which is the common method, and is adopted by the anterior researchers. Just as it is shown in Fig. 11, the aberration will be too large to be corrected totally for myopia above 3 diopters (PV value of the aberration is approximately 20λ).

5. Conclusions

An adaptive optical system for retina imaging has been build. We used a high-resolution LCOS as the wave-front aberration corrector and a Shack–Hartmann wave-front sensor as the aberration detector. The system was designed for eyes with good vision and for myopia eye below 5 diopters. An equivalent scale model eye is constructed as the imaging object. Our experiment result demonstrates that the system can perfectly correct the aberration when the diopter is below 6. Even if the depth of view of the eye varies from -30 to 30 mm, the RMS value after correction can reduce to 0.08λ or smaller for 532 nm wavelength and 6 mm pupil. Furthermore, we can deduce that if the target light source is set at 125 mm away from the eye (i.e. the first image of the retina will focus at the position 125 mm before the eye), the system could be applied to the myopia eye below 8 diopter, even to 10 diopter.

The main differences between the model eye and the real eye are that the dynamics of the real eye aberration and the high-order wave-front distortions. But the dynamic variation of the eye aberration is slow and small. The total wave-front variance produced by high-order aberration for the real eye is usually smaller than $0.3D$ [18]. And the high-resolution LCOS (1024×768 pixels) is able to compensate high-order distortion [15,16]. So it can be concluded that the method will be competent for the real human eye although the experiment is only based on a simple model eye.

Acknowledgments

This work is supported by the National Natural Science Foundation (No. 60578035, No. 50473040, No. 60736042) and the Science Foundation of Jilin Province (No. 20050520, No. 20050321-2).

References

[1] M.S. Smirnov, Biophysics 6 (1961) 766.
[2] H.C. Howland, B. Howland, J. Opt. Soc. Am. A 67 (1977) 2873.
[3] J. Liang, B. Grimm, S. Goelz, J. Opt. Soc. Am. A 11 (1994) 1949.
[4] J. Liang, D.R. Willianms, D.T. Miller, J. Opt. Soc. Am. A 14 (1997) 2884.
[5] M. Glanc, E. Gendron, F. Lacombe, D. Lafaille, Opt. Commun. 230 (2004) 225.
[6] E.j. Fernandez, I. Iglesias, P. Artal, Opt. Lett. 26 (2001) 746.
[7] Ning Ling, Yudong Zhang, et al., Proc. SPIE 4825 (2002).
[8] Jason Porter, Hope M. Queener, Julianna E. Lin, Adaptive Optics For Vision Science, Wiley-Interscience Publication, 2006.
[9] Jose Francisco, Castejon-Mochon, et al., Vision Res. 42 (2002) 1611.
[10] Patricia A. Piers, Silvestre Manzanera, J. Cataract Refract. Surg. 33 (2007) 1721.
[11] L.N. Thibos, A. Bradley, Optom. Vision Sci. 74 (1997) 581.
[12] P.M. Prieto, E.J. Fernandez, S. Manzanera, P. Artal, Opt. Express 12 (2004) 4059.
[13] T. Shirai, Appl. Opt. 41 (2002) 4013.
[14] W. Lotmar, J. Opt. Sac. Am 61 (11) (1971) 1522.
[15] L. Hu, L. Xuan, Y. Liu, Z. Cao, Opt. Express 12 (2004) 6403.
[16] Q. Mu, Z. Cao, L. Hu, Li. Xuan, Opt. Express 14 (2006) 8013.
[17] Warren J. Smith, Modern Optical Engineering, R.R. Donnelley and Sons Company, 2000.
[18] Antonio Guirao, Jason Porter, David R. Williams, J. Opt. Soc. Am. A 19 (2002) 1.